Liquid Crystals
Publication details, including instructions for authors and subscription information:
http://www.informaworld.com/smpp/title~content=t713926090

Electric field induced birefringence in a ferroelectric liquid crystal

M. Conradi; A. V. Kityk; M. Skarabot; R. Blinc; I. Musevic

Online publication date: 06 August 2010

To cite this Article Conradi, M. , Kityk, A. V. , Skarabot, M. , Blinc, R. and Musevic, I.(1999) 'Electric field induced birefringence in a ferroelectric liquid crystal', Liquid Crystals, 26: 8, 1179 — 1184

To link to this Article: DOI: 10.1080/026782999204200

URL: http://dx.doi.org/10.1080/026782999204200

Electric field induced birefringence in a ferroelectric liquid crystal

M. CONRADI†, A. V. KITYK†, M. ŠKARABOT†, R. BLINC†‡
and I. MUŠEVIČ†‡*

†J. Stefan Institute, Jamova 39, 1000 Ljubljana, Slovenia
‡Faculty for Mathematics and Physics, University of Ljubljana, Jadranska 19,
1000 Ljubljana, Slovenia

(*Received 29 December 1998; in final form 16 February 1999; accepted 6 March 1999*)

We have measured the d.c. electric field dependence of the birefringence and conoscopic images for the smectic C* phase of a partially racemized ferroelectric chiral smectic liquid crystal CE-8. The experiments were performed using 50 μm thick homeotropic cells with lateral electrodes which created a d.c. electric field parallel to the smectic layers. The observed field induced birefringence shows a characteristic step-like behaviour which is due to the step-by-step unwinding of the helical structure in a sample with finite dimensions along the helical axis. In conoscopic observations we observe that these steps are associated with moving disclination lines that traverse the sample in the direction of the smectic layers. The observed electric field dependence of the birefringence is discussed in terms of the soliton-like unwinding of helical smectic structures and compared with the predictions of the Landau theory. A qualitatively good agreement is obtained.

1. Introduction

In recent years conoscopic observations of polar smectic phases in an external electric field have often been used to identify different liquid crystalline phases [1, 2]. The shape and evolution of the conoscopic images in an external electric field provide a clue to the identification of different intermediate phases of antiferroelectric liquid crystals. Because the conoscopic image contains information on the birefringent properties of a given phase, these conoscopic observations were sometimes used to extract data on the electric field induced birefringence and biaxiality [2]. The birefringence resolution of conoscopic experiments has been traditionally limited due to poor spatial resolution of the shape of the conoscopic figure. It seems therefore worthwhile to re-examine the electric field induced birefringence of these new phases with newly available high resolution optical techniques, which can give additional valuable information for structural identifications. This work was initiated by the lack of systematic and quantitative comparisons of the electric field induced birefringence and conoscopic images in well known systems, such as the chiral ferroelectric smectic C* phase. It could serve as a starting point for the understanding of results from similar experiments on intermediate phases with unknown structure and unknown response to an electric field.

The unwinding of the helical smectic C* phase in an external d.c. electric field has been studied both theoretically and experimentally for a sample of infinite length along the helical axis [3–5]. The helical period and static susceptibility have been predicted to diverge logarithmically close to the critical field for the helical unwinding, which seems to be in contradiction with experimental results [6, 7]. The d.c. electric field unwinding of the smectic C* with finite dimensions along the helical axis has been considered by Urbanc *et al.* [8]. This analysis showed that for a thin sample of only several helical periods, the unwinding of the helix proceeds via a series of finite jumps. Each individual jump corresponds to the exclusion of a single domain wall from the sample. It has also been shown that for a sample thickness of more than typically 10 helical periods, the discrete helical jumps follow the field dependence of the helical period that is calculated for an infinite sample (see figure 2 of [8]). The optical properties of the helicoidally modulated smectic C* phase are on the other hand well understood. It has been shown theoretically and confirmed experimentally that a simple perturbative approach to the optics of birefringent modulated phases can explain the experimental observations [9]. This approach has been used to explain quantitatively the magnetic field induced biaxiality in a ferroelectric liquid crystal in a transverse magnetic field.

The paper is organized as follows. We first describe the behaviour of the ferroelectric smectic C* phase in a transverse d.c. electric field within the CAA approximation. This is followed by a brief calculation of the electric field induced birefringence within the first order

*Author for correspondence; e-mail: igor.musevic@ijs.si

Journal of Liquid Crystals ISSN 0267-8292 print/ISSN 1366-5855 online ©1999 Taylor & Francis Ltd
http://www.tandf.co.uk/JNLS/lct.htm
http://www.taylorandfrancis.com/JNLS/lct.htm

approximation to the optical properties of inhomogeneous birefringent media. The experiment and the experimental results are described and discussed in §3, which is followed by conclusions in §4.

2. Theory

We first briefly review the behaviour of a bulk ferroelectric smectic C* phase in a transverse d.c. electric field applied perpendicular to the helical axis [8]. The sample is aligned homeotropically, the normal to the smectic layers is along the z-axis and is perpendicular to the confining surfaces. The electric field **E** is applied along the y-axis, $E=(0, E, 0)$. In the constant amplitude approximation (CAA) we consider only the phase-dependent part of the free energy

$$g(z)=\frac{1}{2}K_3\theta_o^2\left(\frac{\mathrm{d}\Phi}{\mathrm{d}z}\right)^2-\Lambda\theta_o^2\frac{\mathrm{d}\Phi}{\mathrm{d}z}-EP_o\cos\Phi. \quad (1)$$

Here, K_3 is the torsional elastic constant, Λ is the coefficient of the Lifshitz term, θ_o and P_o are the spontaneous tilt and polarization, respectively, and $\Phi(z)$ is the phase profile of the helical structure. In zero field, $\Phi(z)=q_c z$, and the critical wave vector $q_c=2\pi/p_o$ corresponds to the undisturbed helical period p_o. After minimization of the total free energy, one obtains the sine-Gordon equation for the phase profile $\Phi(z)$. Periodic solutions of this equation can be expressed analytically with Jacobi's elliptic functions

$$\Phi(z)=4\arctan\left[\left(\frac{1-h}{1+h}\right)^{1/2}\frac{\mathrm{sn}(u;\tilde{k})}{\mathrm{cn}(u;\tilde{k})}\right]. \quad (2)$$

This phase profile represents a 2π-soliton lattice, which is formed by the linear coupling of electric dipoles to the external electric field. Here, $\mathrm{sn}(u;\tilde{k})$ and $\mathrm{cn}(u;\tilde{k})$ are Jacobi's elliptic sine and cosine, respectively. The argument of these functions is $u=\alpha\tilde{z}$, where $\tilde{z}=z/[(K_3\theta_o^2)/(E_c P_o)]^{1/2}$ is the reduced coordinate, $\alpha=\pi(1+h)q_c/8E(h)$ and the modulus is $\tilde{k}=2\sqrt{h}/(1+h)$. The parameter h determines the degree of deformation of the phase profile $\Phi(z)$. For small h, the profile is plane wave-like, whereas for $h\to 1$, the phase profile tends to a soliton-like modulation. The parameter h is determined from the transcendental equation [10]

$$h=\left(\frac{E}{E_c}\right)^{1/2}E(h). \quad (3)$$

In these expressions, $E(h)$ is the complete elliptic integral of the second kind. The critical electric field E_c, where the ferroelectric phase is unwound, is

$$E_c=\left(\frac{\pi}{4}\right)^2\frac{K_3\theta_o^2 q_c^2}{P_o}. \quad (4)$$

It can be shown [10], that the helical period depends on the electric field,

$$p(E)=p_o\left(\frac{2}{\pi}\right)^2E(h)K(h). \quad (5)$$

Here, p_o is the helical period in zero field and $K(h)$ is the complete elliptic integral of the first kind. It is easy to see that the helical period diverges at the critical field.

The confinement of the sample and, in particular the finite dimensions of the sample along the helical axis have a considerable influence on the static and dynamic behaviour of the smectic C* phase in an external d.c. electric field [9]. It has been shown by Urbanc *et al.* [8], that in this case the helical period does not increase continuously, but rather shows discontinuous jumps, each corresponding to the exclusion of a single 2π domain from the sample. They have also shown that for a sample thickness of more than typically 10 helical periods, the discrete helical jumps follow the field dependence of the helical period that is calculated for an infinite sample.

The optical properties of a helical ferroelectric smectic C* structure in a transverse d.c. electric field can be considered in the first order approximation to the wave equation [9]. Within this approximation, the optical properties are described by the space-averaged dielectric tensor, which is for the smectic C* phase

$$\varepsilon(z)=\begin{bmatrix}\frac{1}{2}[(\varepsilon_1+\varepsilon_2)+(\varepsilon_3-\varepsilon_2)\sin^2\theta] & 0 & 0\\ 0 & \frac{1}{2}[(\varepsilon_1+\varepsilon_2)+(\varepsilon_3-\varepsilon_2)\sin^2\theta] & 0\\ 0 & 0 & \varepsilon_3-(\varepsilon_3-\varepsilon_2)\sin^2\theta\end{bmatrix}$$
$$+(\varepsilon_3-\varepsilon_2)\sin\theta\cos\theta\begin{bmatrix}0 & 0 & \cos\Phi(z)\\ 0 & 0 & \sin\Phi(z)\\ \cos\Phi(z) & \sin\Phi(z) & 0\end{bmatrix}$$
$$+\frac{1}{2}[(\varepsilon_2-\varepsilon_1)+(\varepsilon_3-\varepsilon_2)\sin^2\theta]\begin{bmatrix}\cos 2\Phi(z) & \sin 2\Phi(z) & 0\\ \sin 2\Phi(z) & -\cos 2\Phi(z) & 0\\ 0 & 0 & 0\end{bmatrix}. \quad (6)$$

The spatially inhomogeneous part of the dielectric tensor has two contributions with two different spatial periods, i.e. pitch and half a pitch, respectively.

When calculating the space-averaged tensor, one needs to know the spatial averages $\langle \sin \Phi(z) \rangle$, $\langle \cos \Phi(z) \rangle$, $\langle \sin 2\Phi(z) \rangle$ and $\langle \cos 2\Phi(z) \rangle$. It is straightforward to show that these averages are equal to zero in the absence of external fields. By symmetry considerations, it is also easy to see that a linear coupling induces finite spatial averages of $\langle \sin \Phi(z) \rangle$ and $\langle \cos \Phi(z) \rangle$. In particular,

$$\langle \cos \Phi(z) \rangle = \left\{ \frac{2}{h^2} \left[1 - \frac{E(h)}{K(h)} \right] - 1 \right\}. \tag{7}$$

Similarly, quadratic coupling, such as for example with a transverse magnetic field, induces finite spatial averages of $\langle \sin 2\Phi(z) \rangle$ and $\langle \cos 2\Phi(z) \rangle$. These effects also have a clear physical interpretation by considering the form of a space-averaged dielectric tensor. For example, a d.c. electric field applied along the y-direction would induce a tensor of the form

$$\langle \varepsilon \rangle = \begin{bmatrix} \varepsilon_{xx} & 0 & \varepsilon_{xz} \\ 0 & \varepsilon_{xx} & 0 \\ \varepsilon_{xz} & 0 & \varepsilon_{zz} \end{bmatrix}. \tag{8}$$

This represents a rotation of an originally diagonal uniaxial tensor around the y-axis. Physically, this represents a rotation of the optical axis around the direction of the external field, which is indeed observed in the experiments. The component ε_{xz} contains the spatial average $\langle \cos \Phi(z) \rangle$, see equation (2), and is

$$\varepsilon_{xz} = (\varepsilon_3 - \varepsilon_1) \sin \theta_o \cos \theta_o \left\{ \frac{2}{h^2} \left[1 - \frac{E(h)}{K(h)} \right] - 1 \right\}. \tag{9}$$

Here, ε_3 is the dielectric constant measured along the molecular long axis and ε_1 is the dielectric constant measured in a transverse direction. Equation (9) therefore allows us to compare the experimentally determined electric field induced birefringence with the predictions of the Landau theory.

3. Experimental results and analysis

The birefringence set-up used in these measurements is a standard high resolution polarimeter, based on a photoelastic modulator, as described elsewhere [11]. The accuracy of the polarimeter is 0.01° of the retardation between the ordinary and the extraordinary wave. In $\approx 50\,\mu$m thick samples, this gives an accuracy of the birefringence of the order of $\delta\Delta n \approx 10^{-6}$, which is high enough to see fine variations of the index of refraction due to electric field induced distortions of the phase profile. The conoscopic set-up was constructed using a high power argon laser, which was polarized and focused by a large numerical aperture objective onto the liquid crystal layer. After the analyser, the conoscopic image was projected on a semi-transparent screen. Here, the conoscopic image was observed with a CCD camera and captured with a video frame grabber into a PC.

We have used a mixture of 35 wt % chiral and 65 wt % racemic CE-8 in the experiments. The smectic A–smectic C* phase transition in our samples was at 366 K. The critical electric field for the unwinding of the helix in this mixture is several hundred volts for an electrode gap of one millimeter. The samples were aligned in 50 μm DMOAP coated glass cells with a good homeotropic alignment. The electrodes were made by etching the ITO conductive layer on the surface of one plate. We could not use copper wire electrodes, as suggested by other authors, because the electric current with copper electrodes was too high and resulted in a rapid deterioration of the cell alignment.

The electric field dependence of the birefringence, as observed at an angle of 30° with respect to the optical axis is shown in figure 1, for different sweep times of the electric field. In all cases, one can see a stepwise increase of the induced birefringence with the electric field. This step-like behaviour is more pronounced close to the critical field, where the helix is expected to change rapidly with the field. We have noted that the number of steps is closely related to the number of the helical periods in the sample. The period of the helix of the mixture is of the order of 5 μm and changes slightly with temperature. The number of helical turns in the sample is close to 10, which is in qualitative agreement with the number of steps observed in the experiment. The electric field induced birefringence shows a significant dependence on the time of the sweep of the electric field, although the overall features remain unchanged. For short sweeps, one can see a characteristic 'tail' of the birefringence at large fields. This means that the birefringence does not change as rapidly with the field as expected from theory. Consequently, the measured 'apparent critical electric field' is always larger than the theoretically estimated field. This indicates that the experiments were not performed in equilibrium as there was not enough time to allow for thermal equilibration.

The stepwise behaviour of the electric field induced birefringence is observed throughout the temperature range of the ferroelectric phase, as shown in figure 2. The critical electric field increases with decreasing temperature, as expected due to the increasing ratio of θ_o^2/P_o in equation (4). We have also calculated the electric field induced birefringence following equation (9) for the space-averaged dielectric tensor. The calculated change of the birefringence due to the rotation of the dielectric tensor, equation (8), under the influence of the electric field is shown in the inset to figure 2, together with the data for the two experimental runs.

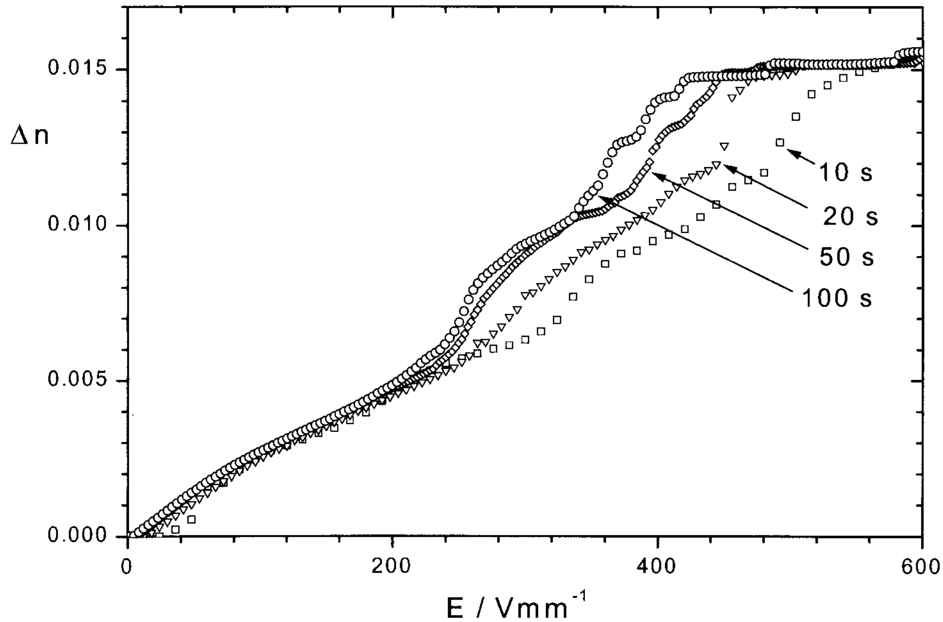

Figure 1. The electric field dependence of the birefringence in a 35:65 wt % mixture of chiral and racemic CE-8, as observed at an angle of 30° with respect to the optical axis for different times of the sweep of the field. The measurement was performed at $T_c - T = 25$ K. Note the characteristic 'tail' for short runs and the clear presence of steps for longer experimental runs.

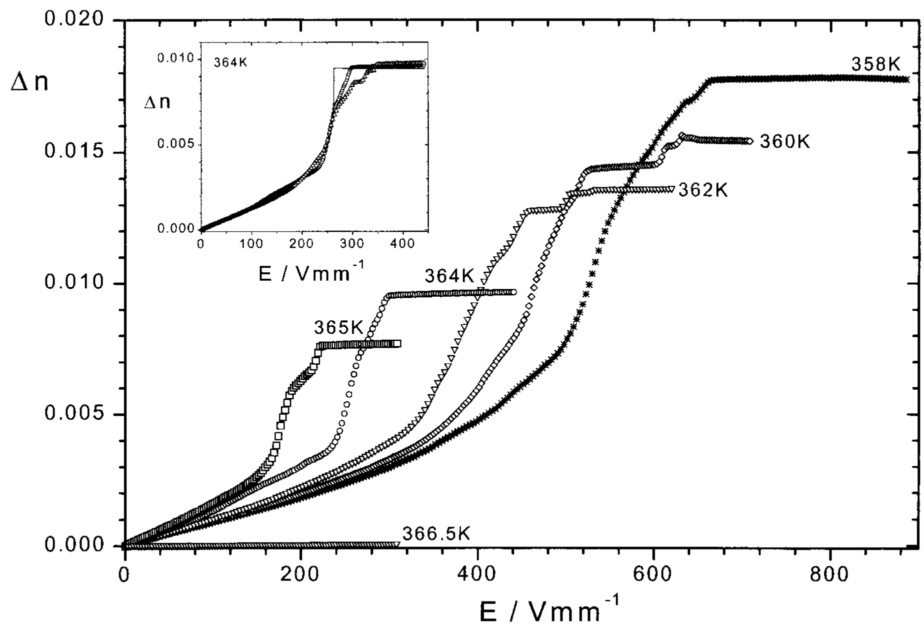

Figure 2. The electric field dependence of the birefringence in a 35:65 wt % mixture of chiral and racemic CE-8, as observed at an angle of 30° with respect to the optical axis at different temperatures. The duration of the field sweep was 100 s. The inset shows a fit of data from two experimental runs to the equation (9), using the equations (3) and (4). The tilt angle and birefringence were determined directly in an independent experiment.

The agreement is only qualitatively good at low fields, whereas close to the critical field, the experimental data significantly deviate from the theoretical predictions. We think that this deviation is because the field sweeps were performed in a time that was too short to allow for complete thermal equilibration.

The step-like behaviour of the birefringence suggests that the helical unwinding proceeds in individual steps. During each step, a single or multiple number of 2π domain walls is presumably squeezed out of the sample. This conjecture is further supported if we calculate the expected change of the birefringence of the sample, when a single 2π domain is squeezed-out. Using equation (2) for the phase profile, we have calculated that a single 2π domain wall contributes a birefringence of the order of $\Delta n \approx 1.5 \times 10^{-3}$, when the electric field is close to the critical field. This is in reasonable agreement with experiment, which shows birefringence jumps of the same order of magnitude. We should also note that the steps are sometimes more and sometimes less pronounced, as can be seen from the inset to figure 2.

The conjecture of a step-by-step-like unwinding of the ferroelectric structure in an external electric field was also probed by conoscopic imaging. During the field sweep, conoscopic images were captured at regular time intervals, thus capturing a movie of the helical unwinding. As shown in a sequence of conoscopic images in figure 3, the image first tilts as a whole in a plane perpendicular to the direction of the electric field. This is followed by the passage of a series of 'fronts' over the field of view, as shown in figure 3(*c*). Finally, above the critical field, we have a typical biaxial conoscopic image of an unwound ferroelectric phase. What is here interesting is the presence of 'fronts', which appear at the edge of a sample and then travel at a uniform speed throughout the field of view. These fronts are correlated with the step-like increase of the birefringence and are very important in the mechanism of the unwinding of helical structures. We conjecture that somehow the dislocations are created at the edge of the sample. These dislocations then travel through the smectic structure and annihilate a single 2π domain wall of the distorted ferroelectric structure. As a result, the number of helical turns in the sample is reduced by one and the structure is again in thermal equilibrium. Upon increasing the electric field, the mechanism appears again and we have a step-by-step increase of the birefringence. These observations indicate that the helical unwinding in thin cells with a finite ratio of p_0/d is of a nucleation character. The unwinding proceeds via a series of 'fronts' that annihilate single 2π domain walls. A similar mechanism was observed by Glogarova *et al.* for thin planar cells [12].

4. Conclusions

In this paper, the following observations concerning the behaviour of helicoidally modulated polar smectic structures in an external d.c. electric field have been reported:

(i) The unwinding of helical structures in an external d.c. electric field is a very slow process. We estimate that the field sweep up to critical field should always be longer than several minutes or even tens of minutes. For shorter field sweeps, metastable states can be clearly observed close to the critical field and the experimentally determined critical field is always larger than the true equilibrium critical field.

(ii) The unwinding of the helical structure always proceeds in a step-like manner. This is most

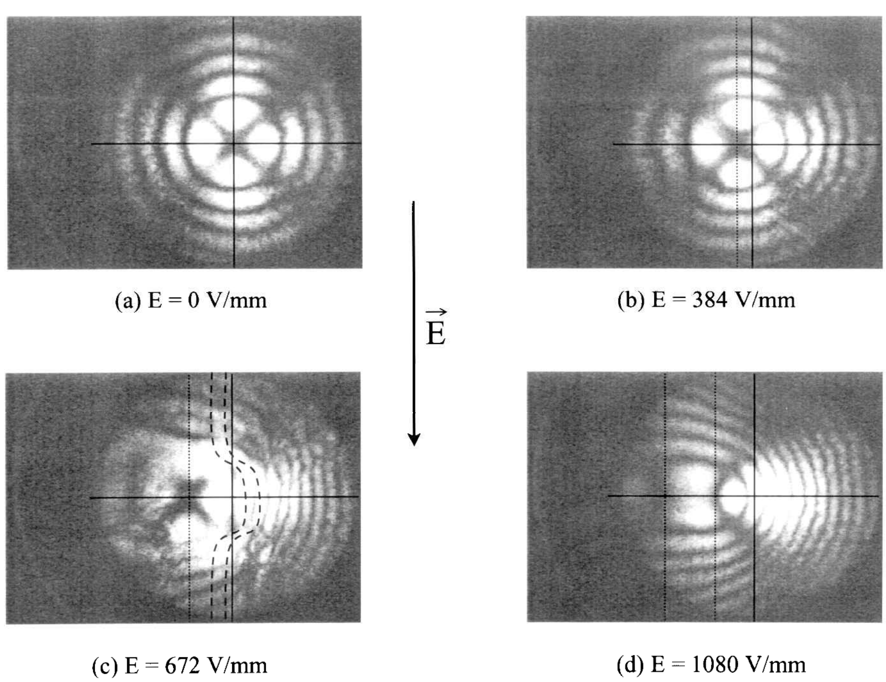

Figure 3. The sequence of conoscopic images, as obtained with a 35:65 wt % mixture of chiral and racemic CE-8 at a temperature $T_c - T = 0.5$ K. The electric field was increased at a rate of 36 V mm^{-1} s^{-1}. The shift of the conoscopic figure is accompanied by the passage of clearly observable disclination lines (dashed lines) that correspond to the unwinding of the helical structure.

obviously seen in thin samples with a large ratio of the helical period to the sample thickness p_o/d, but should be present in thick samples as well. Each step in this process corresponds to the annihilation of a single or a multiple number of 2π domain walls.

(iii) The annihilation of a domain wall, which increases the helix by a single step, proceeds via a movement of a disclination wall that is usually nucleated at the edge of a sample.

We believe that the above results are generally valid for polar smectics and should be taken into account also in experimental studies of antiferroelectric and intermediate phases of antiferroelectric liquid crystals in external electric fields.

References

[1] Gorecka, E., Chandani, A. D. L., Ouchi, Y., Takezoe, H., and Fukuda, A., 1990, *Jpn. J. appl. Phys.*, **29,** 131.

[2] Isozaki, T., Fujikawa, T., Takezoe, H., and Fukuda, A., 1993, *Phys. Rev. B*, **48,** 13 439.

[3] Hudak, O., 1983, *J. Phys., Paris*, **44,** 57.

[4] Dmitrienko, V. E., and Belyakov, V. A., 1980, *Zh. eksp. teor. Fiz.*, **78,** 4.

[5] Urbanc, B., Žekš, B., and Carlsson, T., 1991, *Ferroelectrics*, **113,** 207.

[6] Bahr, Ch., Heppke, G., and Sharma, N. K., 1987, *Ferroelectrics*, **76,** 151.

[7] Pavel, J., Glogarova, M., and Bawa, S. S., 1987, *Ferroelectrics*, **76,** 221.

[8] Kutnjak-Urbanc, B., Žekš, B., and Rovšek, B., 1993, *Liq. Cryst.*, **14,** 999.

[9] Muševič, I., Žekš, B., Blinc, R., and Rasing, Th., 1995, *Liquid Crystals in the Nineties and Beyond*, edited by S. Kumar (World Scientific), chap. 6.

[10] Kutnkak-Urbanc, B., 1993, PhD. thesis, University of Ljubljana, 1993.

[11] Škarabot, M., Čepič, M., Žekš, B., Blinc, R., Heppke, G., Kityk, A. V., and Muševič, I., 1998, *Phys. Rev. E*, **58,** 575.

[12] Glogarova, M., Lejček, L., Pavel, J., Janovec, V., and Fousek, J., 1983, *Mol. Cryst. liq. Cryst.*, **91,** 309.